

Vacuum-Packaged Suspended Microchannel Resonant Mass Sensor for Biomolecular Detection

Thomas P. Burg, *Member, IEEE*, Amir R. Mirza, Nebojsa Milovic, Christine H. Tsau, George A. Popescu, John S. Foster, and Scott R. Manalis

Abstract—There is a great need in experimental biology for tools to study interactions between biological molecules and to profile expression levels of large numbers of proteins. This paper describes the fabrication, packaging and testing of a resonant mass sensor for the detection of biomolecules in a microfluidic format. The transducer employs a suspended microchannel as the resonating element, thereby avoiding the problems of damping and viscous drag that normally degrade the sensitivity of resonant sensors in liquid. Our device differs from a vibrating tube densitometer in that the channel is very thin, which enables the detection of molecules that bind to the channel walls; this provides a path to specificity via molecular recognition by immobilized receptors. The fabrication is based on a sacrificial polysilicon process with low-stress low-pressure chemical-vapor deposited (LPCVD) silicon nitride as the structural material, and the resonator is vacuum packaged on the wafer scale using glass frit bonding. Packaged resonators exhibit a sensitivity of $0.8 \text{ ppm}/(\text{ng} \cdot \text{cm}^2)$ and a mechanical quality factor of up to 700. To the best of our knowledge, this quality factor is among the highest so far reported for resonant sensors with comparable surface mass sensitivity in liquid. [1720]

Index Terms—Biomedical transducers, chemical transducers, density measurement, Q factor, mass sensor, microbalance, vacuum packaging.

I. INTRODUCTION

MICROFABRICATED transducers enable the detection of biomolecules in microfluidic systems with nanoliter size sample volumes. Their integration with microfluidic sample preparation into lab-on-a-chip devices can greatly leverage

experimental efforts in systems biology and pharmaceutical research by increasing analysis throughput while dramatically reducing reagent cost. Microdevices can also lead to robust and miniaturized detection systems with real-time monitoring capabilities for point-of-use applications.

Sensors that detect unlabeled biomolecules typically measure changes in a physical property, such as charge, refractive index, surface stress, or mass at a solid-liquid interface. To provide specificity, immobilized receptors preferentially bind the target molecules of interest, altering the properties of the surface and generating a signal. Unlike conventional protein microarrays, this scheme does not require a secondary antibody or fluorescent labeling of the target molecules. Therefore, label-free detection technologies enable experiments in which labeling would interfere with the binding reaction, or in which real-time measurements of the binding kinetics are of interest. In addition, no secondary antibody is required for detection and hence label-free methods are applicable in many cases where a fluorescent sandwich assay cannot be used.

Surface plasmon resonance (SPR) [1], [2] and the quartz crystal microbalance (QCM) [3], [4] are currently the two most widely employed methods for label-free protein interaction analysis, with applications ranging from fundamental research in systems biology to drug discovery and quality control. Laboratory instruments based on SPR and QCM are commercially available, however these two principles are not easily amenable to miniaturization and batch fabrication.

The three main classes of microfabricated sensors for biochemistry can be classified as electronic, optical and mechanical transducers, all of which have specific advantages and limitations. Electronic field-effect devices can be highly sensitive to binding of charged molecules regardless of molecular weight, however due to charge screening these sensors require low ionic strength solutions and tight binding of ligands to the surface. [5], [6] Integrated optical sensors rely on the measurement of refractive index in the evanescent field of planar waveguides, which generally limits the thickness of the sensitive layer to less than 100 nm and requires intricate alignment of external optical components to the microfabricated part. [7]–[9] Micromechanical surface stress sensors have recently been the subject of many research efforts, in part because of their simplicity and high sensitivity in certain assays. [10]–[12] Since surface stress depends on a number of physical properties of the interface, such as charge, hydrophobicity, or steric hindrance between adsorbed molecules, sensitivity to different target molecules can

Manuscript received November 21, 2005; revised April 3, 2006. This work was supported by the National Institutes of Health (Center for Cell Decision Process GM-68762 and R21 EB003403-01), U.S. Army Research Office (Institute for Collaborative Biotechnologies DAAD19-03-D-004), and Air Force Office of Sponsored Research (FA9550-04-1-0049). Devices were fabricated in the MIT Microsystems Technology Laboratories and at Innovative Micro Technology. Subject Editor G. K. Fedder.

T. P. Burg, N. Milovic, and C. H. Tsau are with the Division of Biological Engineering, Massachusetts Institute of Technology, Cambridge, MA 02139 USA.

A. R. Mirza and J. S. Foster are with the Innovative Micro Technology, Santa Barbara, CA USA 93117 USA.

G. A. Popescu is with the Media Laboratory, Massachusetts Institute of Technology, Cambridge, MA 02139 USA.

S. R. Manalis is with the Division of Biological Engineering, Massachusetts Institute of Technology, Cambridge, MA 02139 USA. He is also with the Department of Mechanical Engineering, Massachusetts Institute of Technology, Cambridge, MA 02139 USA (e-mail: scottm@media.mit.edu).

Color versions of Figs. 1–6 and 8–10 are available online at <http://ieeexplore.ieee.org>.

Digital Object Identifier 10.1109/JMEMS.2006.883568

vary widely. In addition, the need for different surface functionality on the top and bottom side of the device complicates assay development.

Another class of micromechanical transducers is formed by micromechanical resonators whose natural frequency provides a measure of mass adsorbed to their surface. Resonant mass sensors have been highly successful for chemical sensing in gaseous environments. [13]–[15] In liquids, however, the mass sensitivity and frequency resolution of resonant sensors is degraded by the low quality factor (Q) and large effective mass that is induced by viscous drag. While certain designs have the potential to greatly alleviate these limitations, their sensitivity is still inferior to air or vacuum based resonators. [16], [17] To overcome this problem, various groups have employed the ‘dip and dry’ method, by which the resonance frequency is measured in air before and after the device has been exposed to the sample. [18], [19] To ensure reliability, great care must be taken to avoid contamination of the resonating element. Furthermore, the technique does not allow real-time measurements for studying binding kinetics. For some assays, mass enhancing labels can be used to increase the signal-to-noise ratio in liquid at the expense of additional sample preparation and experimental complexity. [20]

We have recently demonstrated a new type of sensor known as the suspended microchannel resonator (SMR) that effectively addresses the problems of a limited quality factor and large effective mass in liquids. [21] In SMR detection, target molecules flow through a vibrating suspended microchannel and are captured by receptor molecules attached to the interior channel walls. In our previous work, devices were packaged on the chip-scale with poly(dimethylsiloxane) (PDMS) and the resonator was excited with an externally aligned electrode. While this configuration was sufficient for demonstrating the SMR concept, it was tedious to assemble, the air permeability of PDMS did not allow packaging in vacuum where frequency resolution is optimal, and mechanical disturbances of the external electrode limited measurement stability and precision. Here we address these drawbacks by introducing the fabrication and wafer-level vacuum packaging of SMRs with integrated electrodes. We show that the Q is increased by more than six times and is not degraded by the presence of solution inside the SMR. The high quality factor enables a short-term frequency stability of one part per million (ppm), and the glass package provides a microenvironment that prevents pressure and humidity fluctuations from affecting the resonance frequency. As a result, we have been able to improve frequency stability on the time scale of thirty minutes by five times compared to our previous work, which is a crucial step towards detecting slow binding molecules at low concentrations.

II. THEORY

A. Device Concept

Fig. 1 illustrates the principle by which the binding of biological molecules to the inside walls of a suspended microfluidic channel is transduced into a frequency signal. The suspended fluid channel constitutes a micromechanical resonator, in which

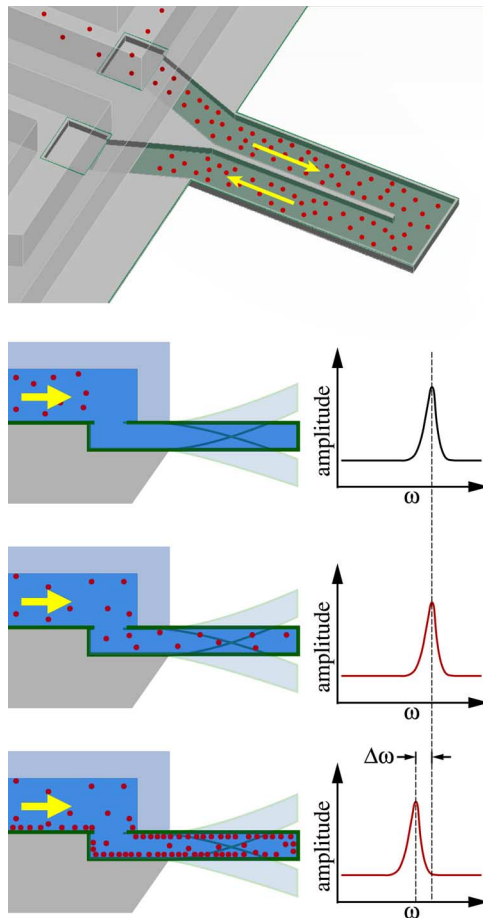


Fig. 1. Molecules binding to the inside walls of a suspended microchannel can be detected by the change in resonance frequency: (1) Before the sample is injected, the resonator is filled with pure buffer solution. (2) If the resonator volume is small, the presence of a dilute sample does not yield a measurable frequency shift. (3) Only molecules that adsorb to the surface while being continuously replenished by the flow can build up a detectable amount of mass.

both the spring constant k and the total effective mass m^* determine the mechanical resonance frequency

$$\omega_0^2 = \frac{k}{m^*}. \quad (1)$$

The effective mass is composed of the fixed mass of the channel walls, the liquid contained inside the channel, and the mass of any adsorbed matter present on the channel walls. If the surface area-to-volume ratio of the channel is large, then the contribution of mass adsorbed to the channel walls is significant. Proteins can be detected by this method since their mass density in aqueous solution is approximately $1.3\text{--}1.4\text{ g/cm}^3$, [22], [23] which is higher than the density of the pure buffer ($\sim 1\text{ g/cm}^3$). If the channel surfaces are derivatized with biological receptors, proteins that bind to the receptors get depleted from the solution and accumulate on the walls as they are continuously replenished by the flow of sample through the device. It is therefore possible to detect the presence of specific target molecules, even if the concentration of these molecules in solution is too low to be directly measured by the change in bulk density.

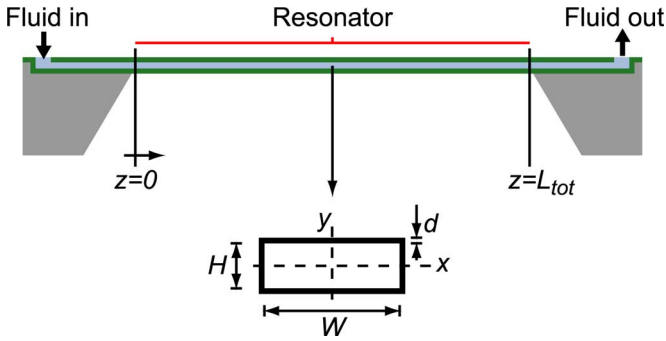


Fig. 2. Parameters describing the geometry of an arbitrarily shaped suspended microchannel. The z -axis measures the distance from the inlet along the channel. The channel is assumed to have a constant cross section of width W and height H , and the wall thickness is denoted by d .

B. Sensor Design

For a long and thin suspended microchannel resonator with constant cross section, the mass sensitivity is, to first order, solely a function of the ratio of adsorbed mass to total mass and does not depend on the exact geometry, resonance frequency, or vibrational mode. To show this we consider a suspended microchannel of arbitrary shape, in which the axial position is parameterized as illustrated in Fig. 2. Assuming pure bending, the displacement field of a vibrational mode is represented by a one-dimensional (1-D) function $u(z)$. Equating the maximum kinetic and the maximum potential energy (W) yields the resonance frequency ω_0

$$\omega_0^2 = \frac{W}{L \int_0^L \frac{1}{2} m_A(z) \cdot u(z)^2 dz} \quad (2)$$

where $m_A(z)$ is the mass per unit length

$$m_A(z) = \int \rho(x, y, z) dx dy. \quad (3)$$

Adsorption of molecules increases m_A by a small amount Δm_A and gives rise to a frequency shift $\Delta\omega$

$$(\omega_0 + \Delta\omega) = \frac{W}{L \int_0^L \frac{1}{2} [m_A(z) + \Delta m_A(z)] \cdot u(z)^2 dz} \quad (4)$$

To first order in Δm_A , $\Delta\omega/\omega_0$ is given by

$$\frac{\Delta\omega}{\omega_0} \approx -\frac{1}{2} \frac{\int_0^L \Delta m_A(z) \cdot u(z)^2 dz}{\int_0^L m_A(z) \cdot u(z)^2 dz} \quad (5)$$

and if the ratio $\Delta m_A(z)/m_A(z)$ is constant we find

$$\frac{\Delta\omega}{\omega_0} \approx -\frac{1}{2} \frac{\Delta m_A}{m_A}. \quad (6)$$

In addition to increasing the mass, chemical reactions can also alter the surface stress at the solid-liquid interface. [10], [24] Since the cantilever resonators considered in this work are clamped only on one end, and because adsorption of molecules occurs symmetrically on the top and bottom surface of the suspended channel, the surface tension term in the potential energy W vanishes to first order. Therefore, surface stress is neglected in this paper. It should be noted, however, that more detailed models based on the specific resonator geometry would need to be used to provide a precise description of this effect.

Equation (6) shows that when molecules adsorb uniformly onto the surface of a resonating microchannel with constant cross section, the resulting relative frequency shift due to mass change is independent of the exact shape of the channel. The channel mass per unit length should be minimized in order to optimize sensitivity, and the geometry and mode structure can be chosen to maximize the quality factor and yield high-frequency resolution.

Receptor affinity and surface chemistry determine the density of adsorbed molecules in any given experiment. We are therefore interested in maximizing the relative frequency shift produced by a given amount of added mass per unit area, or equivalently, we seek to maximize the ratio

$$\frac{L}{m_A} = \frac{2(H+W)}{\rho_{H_2O}HW + 2\rho_{wall}d(W+H+2d)} \quad (7)$$

where $L = 2 \cdot (H+W)$ denotes the length of the solid-liquid interface shown in Fig. 2. For a fixed channel width W , the sensitivity increases with decreasing fluid layer thickness and with decreasing wall strength. If $H, d \ll W$, the width does not significantly affect the ratio L/m_A , and W is limited in practice by the need for mechanical robustness and potentially by geometrical requirements of the deflection sensor. For example, the optical system used in our experiments requires focusing a laser beam on the suspended microchannel, which therefore needs to be at least as wide as the spot diameter. If capacitive detection is used, it is also desirable to maximize the sensor width in order to increase the signal. Ultimately, the mechanical strength and the risk of stiction limit the width of the channel and the aspect ratio.

To determine the channel height, a trade-off must be made between mass sensitivity, flow rate, and fabrication complexity: While a very thin channel has low mass and therefore high sensitivity, the flow rate at practical operating pressures is low and mass transport limitations become a concern. [25] Furthermore, sensitivity gains are marginal once the height is less than the wall thickness, because at this point the device mass is dominated by the mass of the solid structure. The sacrificial polysilicon process used to fabricate the channels is most robust for a channel depth in the range of several hundred nanometers to a few microns. This range is determined by the ability to deposit a thick sacrificial polysilicon layer, and by the precision of the surface planarization (cf. Section III-A). Based on these constraints we designed channels that are 20 μm wide and 1 μm tall with 800 nm thick walls, as shown in the cross-section in Fig. 7 (see Section IV). The suspended channel has the shape of a U, forming a 300- μm -long and 63- μm -wide hollow cantilever

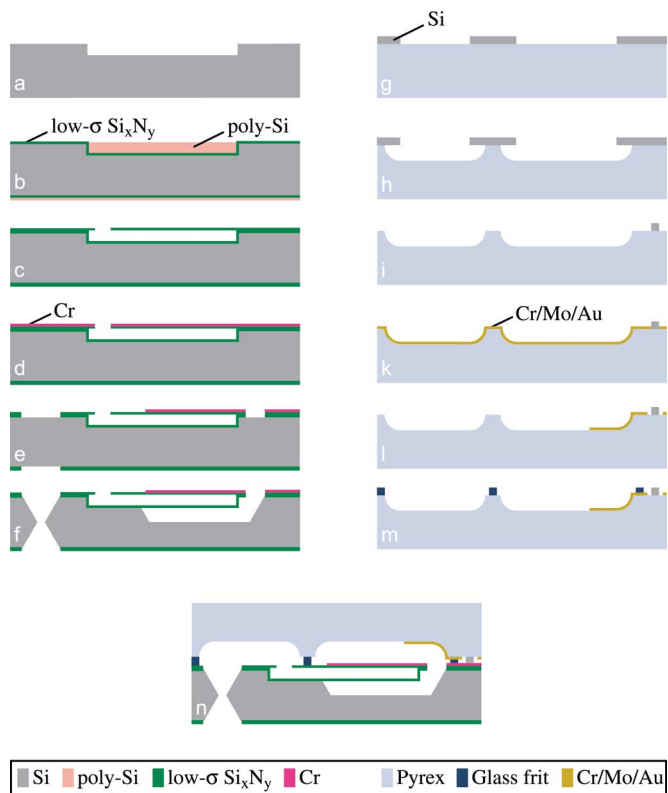


Fig. 3. Fabrication and packaging process: Suspended microchannels with a 1- μm fluid layer and 800-nm-thick silicon nitride walls are fabricated using a sacrificial polysilicon process and chemical mechanical polishing. Following the release, the device wafer is glass frit-bonded under vacuum to a Pyrex capping wafer.

beam. Given the high torsional stiffness of this beam, Coriolis force induced twisting due to the longitudinal mass transport is below the detection limit of our displacement sensor under all practical operating conditions.

III. FABRICATION AND PACKAGING

A. Fabrication Process and Wafer-Level Packaging

High sensitivity to surface bound mass in a hollow resonator requires a large ratio of surface area to channel volume and wall thickness. The devices presented in this paper were fabricated using a polysilicon sacrificial layer and low-stress low-pressure chemical-vapor deposited (LPCVD) silicon nitride as the structural material. This material combination enables the release of very long hollow channels with thin walls [26].

First, the channels were etched to a depth of 1 μm using reactive ion etching (RIE) in sulfur hexafluoride [see Fig. 3(a)]. The wafers were then coated with 800 nm low-stress LPCVD silicon nitride followed by 1.5 μm LPCVD polysilicon. Low-stress silicon nitride was deposited from a 10:1 ratio of dichlorosilane and ammonia in an SVG/Thermco 7000 vertical thermal reactor at 775 $^{\circ}\text{C}$ and 250 mTorr. The polysilicon was subsequently removed from the wafer surface by CMP, so that only the etched features remained filled [see Fig. 3(b)]. After this planarization, another layer of low-stress LPCVD silicon nitride was deposited to close the polysilicon filled microchannels.

Finally, access holes (60 μm \times 30 μm , cf. SEM inset in Fig. 4) were etched into the top nitride, and the polysilicon was dissolved in hot potassium hydroxide (KOH), as illustrated in Fig. 3(c). Using a six molar solution of KOH in water at a temperature of 80 $^{\circ}\text{C}$ the 2-mm-long channels were completely released after approximately 20 h. Stiction was prevented by the high stiffness of the 20 μm wide and 800-nm-thick nitride diaphragm that formed the top of the channel. After the release, a 50-nm layer of chromium was deposited by ion beam deposition [see Fig. 3(d)]. The purpose of the chromium layer is to provide high reflectivity for the optical readout and, at the same time, to serve as an electrode for electrostatic actuation. The chromium was patterned in order to minimize stress on the resonator and to remove the metal from all areas that would later be in contact with the sample fluid. We subsequently dry etched through both silicon nitride layers to define the resonator outline and the location of through-wafer holes for sample delivery. The backside of the wafers was also patterned and etched in the same step, thus enabling etching of the fluid vias from both sides [see Fig. 3(e)]. Finally, the resonators were released by bulk micromachining in tetramethylammonium hydroxide (TMAH), which is compatible with chromium metallization [see Fig. 3(f)].

The first level packaging for the suspended microchannel resonators was done on the wafer scale: A glass wafer providing microfluidic channels as well as electrical interconnects for electrostatic actuation was attached to the device wafer by glass frit bonding. Fabrication of the glass capping wafer required etching deep (~ 50 μm) recesses to form microfluidic channels and cavities for the resonators. Furthermore, electrodes for electrostatic actuation needed to be integrated, and hard spacers of ~ 20 μm height had to be formed to limit the compression of the glass frit during bonding. The mask for the deep channel etch in hydrofluoric acid (HF) was formed by a silicon wafer which was first anodically bonded to the glass, then etched back to 20 μm in potassium hydroxide and patterned using deep-reactive ion etching (DRIE) [see Fig. 3(g)]. After the deep glass etch [see Fig. 3(h)], the masking layer was further reduced by DRIE to leave only a sparse distribution of silicon islands; these formed the hard spacers required by the bonding process [see Fig. 3(i)]. Last, a gold film with adhesion layer was deposited [see Fig. 3(k)] and patterned [see Fig. 3(l)], and the glass frit was silk-screen printed onto the substrate (Fig. 3(m)). Patterning of the metal electrodes in the deep recess was accomplished by using thick negative tone photoresist. The device and the capping wafer were bonded under vacuum [see Fig. 3(n)] and could then be die sawed without damaging the resonators.

Fig. 4 shows a top view of the cantilever resonator. The glass above the beam is recessed by ~ 50 μm and carries an L-shaped gold trace for electrostatic excitation. The white areas in the picture are chromium coated and connect to a common ground contact at the bottom of the chip. Shown in the inset is an atomic force microscope scan of the surface topography across the 20 μm wide buried microfluidic channel. The depression of the channel surface is a result of the CMP process: Deformation of the polishing pad and the higher removal rate of polysilicon compared to silicon nitride result in ~ 125 nm of dishing in the middle of the trench. Since the glass frit that

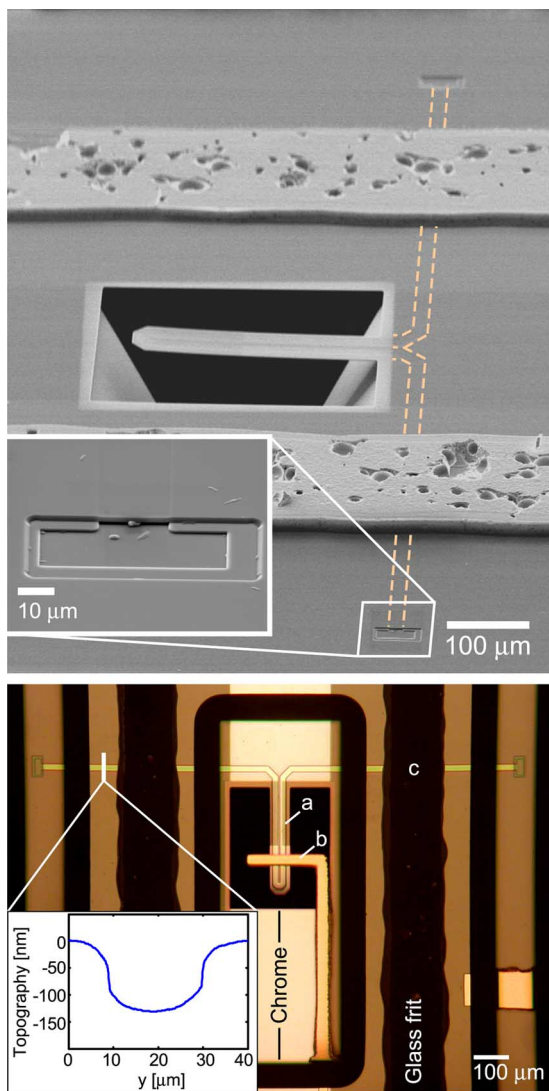


Fig. 4. Top: SEM of cantilever and glass frit after removing the glass lid. The inset shows the channel inlet. Bottom: Optical micrograph of a packaged cantilever resonator. The 300- μm -long beam contains a $1 \times 20 \mu\text{m}$ microfluidic channel (a). An electrode on the glass surface above the cantilever enables electrostatic actuation (b). Glass frit conforms to the surface topography (inset) and does not collapse the thin channel in location (c) during bonding.

seals across the channel at location (c) in Fig. 4 can conform to the surface topography, no further optimization of the CMP process was performed.

All bond pads for electrical contacts are located on the glass lid and get exposed when the silicon wafer is diced. An additional contact to the surface of the metallized resonator is required for a stable electrostatic drive. This connection is made available for wirebonding by transferring the contact from the silicon chip surface to a metal trace on the glass with silver filled epoxy, as shown in Fig. 5(a).

B. Electrical and Microfluidic Interconnects

The wafer-level packaged chips contain a microfluidic network that enables the quick exchange of samples inside the thin resonator channel. Fluids are injected into the chip from the backside via anisotropically etched through holes [see Fig. 5(a)]. Fig. 5(b) illustrates the design of the electronic and fluidic

interface. The sensor chips are attached to an adhesive backed, gold plated printed circuit board (PCB) and wirebonded directly to the board. The assembly is clamped onto a Teflon (PTFE) manifold holding an array of standard 1/32" (0.794 mm) tubes. The holes in the manifold were initially drilled at a smaller nominal diameter (0.711 mm), and the manifold was heated for insertion of the tubes. After cooling to room temperature a leak tight seal was obtained between the through holes in the PTFE block and the outer walls of the tubing. The tubes were made of either Teflon FEP or PEEK. The manifold is sealed against the chip surface with commercially available perfluoroelastomer (SIMRIZ) O-rings, the size of which limits the practical interconnect density to a $3 \text{ mm} \times 3 \text{ mm}$ grid. Our design enables the reversible connection to multiple fluid inlets on a tight space with chemically inert materials. The fluidic seal is reliable and leakage free for pressures up to 150 psi.

IV. EXPERIMENTAL SETUP

An important application of microfabricated biochemical sensors is the label-free and real-time monitoring of binding reactions. Our experimental setup enables a continuous measurement of resonance frequency with high temporal resolution and very high accuracy. Additionally, samples can be seamlessly injected into the sensor without causing any detectable disturbance of the signal.

Resonance frequency is measured in a feedback configuration as shown in Fig. 6. The displacement is detected by measuring the deflection of a laser beam that is focused onto the tip of the cantilever. A second order low-pass filter with a cutoff close to the resonance frequency is used to shift the phase of the signal by 90° , resulting in a total phase of 180° at the resonance frequency. The signal is then amplified and connected to the electrostatic drive, thereby forming an oscillator circuit that tracks the natural frequency of the resonator. The drive electrode is biased at 60 V to increase the efficiency of the electrostatic drive, and the amplifier limits the ac signal amplitude to 10 Vpp. The above method provides high resolution and bandwidth, and, at the same time has a dynamic range that is unlimited for all practical purposes; this means that large jumps in frequency, which occur, for example, during the initial filling of the device, can be monitored with the same accuracy and time resolution as subtle changes resulting from the adsorption of thin protein layers. No external drive signal is needed to sustain the oscillation, since with the feedback loop closed thermal noise is amplified by several orders of magnitude in a narrow band around the resonance frequency. This scheme is identical to what is often referred to in the literature as "Q-control." However, although feedback circuits generally enhance the overall Q by several orders of magnitude, it is the mechanical Q that ultimately determines the frequency stability of the readout. [27]

During measurements we maintain a constant flow of sample through the microfluidic inlet bypass, and the induced pressure drives a small flow through the suspended microchannel resonator. The sample is delivered by an Agilent 1100 capillary HPLC system at a constant flow rate of $5.0 \mu\text{L}/\text{min}$, as illustrated in Fig. 7. A 38.1 cm tube with $75 \mu\text{m}$ inner diameter connected between the outlet of the injection bypass and the waste

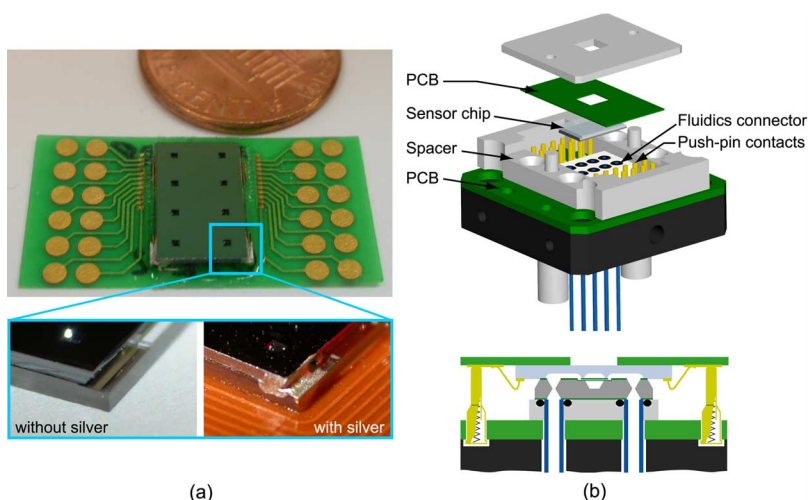


Fig. 5. (a) Bottom view of the sensor chip wirebonded to a PCB. A colloidal silver paste is applied to the corner of the chip to connect the chrome on the resonator surface to a gold trace on the glass lid. (b) The sensor chip is clamped onto a Teflon manifold holding an array of standard 1/32'' OD Teflon tubes. Perfluoroelastomer O-rings seal the manifold to the chip, and an array of spring loaded contacts provides electrical connections to the PCB.

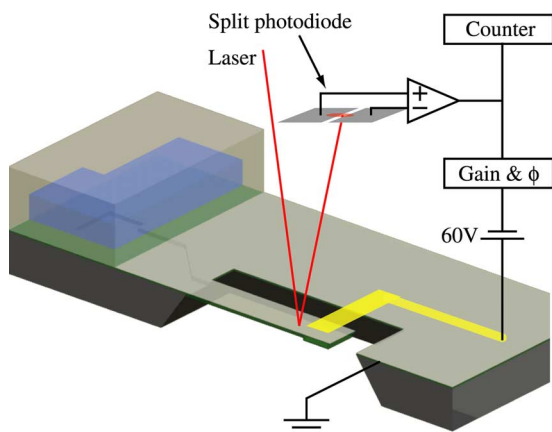


Fig. 6. The vibration of the resonator is measured by the optical lever method. The optical deflection signal is applied to the drive electrode to form an oscillator circuit, and a digital counter measures the oscillation frequency.

reservoir induces a pressure of ~ 6 psi at the resonator inlet, resulting in a flow of ~ 30 pL/s through the thin channel. Since the resonator comprises a volume of only 12 pL plus 14 pL swept volume from the inlet to the base of the suspended channel, it takes less than one second to completely exchange the fluid inside the vibrating beam. The resonator outlet connects to a large bypass channel, which is continuously rinsed at a slow flow rate (~ 1 $\mu\text{L}/\text{min}$) and at low pressure.

V. CHARACTERIZATION RESULTS

A. Resonator Characterization

We characterized the quality factor of the packaged resonator by measuring the frequency response using a network analyzer. The result of this measurement for an empty device is shown in Fig. 8(a) (red curve), with the frequency response of an identical resonator that was not hermetically sealed shown in blue. The reduced damping in the case of the vacuum sealed device results in an improved quality factor of 400 instead of 85. To assess the vacuum level inside the small on-chip cavity, we repeated the

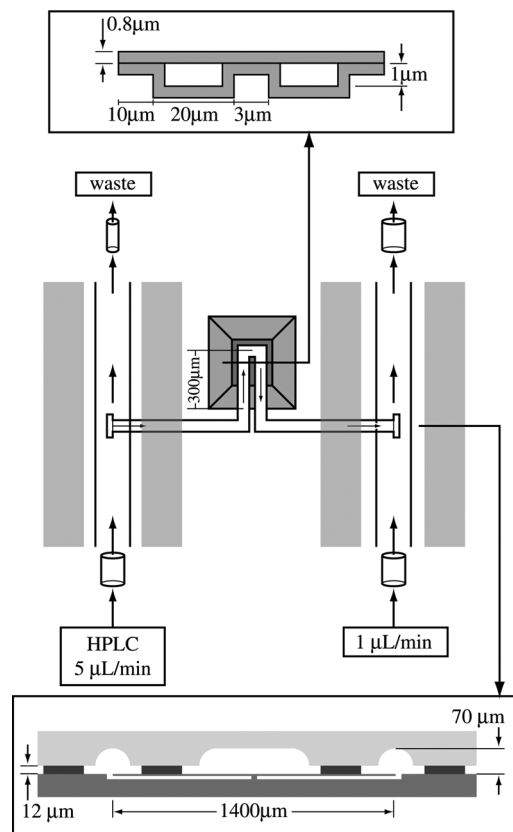


Fig. 7. Microfluidic bypasses enable the quick exchange of samples inside the suspended microchannel. The flow rate through the resonator is controlled by the pressure difference between the inlet and the outlet bypass.

measurement with the not hermetically sealed device inside of a vacuum chamber at pressures ranging from 50 mTorr to one atmosphere, and plotted the quality factor vs. pressure as shown in Fig. 9(b). Comparing the quality factor of the sealed resonator in Fig. 8(a) with Fig. 8(b) then reveals that the vacuum inside the on-chip cavity is on the order of 1 torr, which is typical for glass frit sealed microcavities without getters [28]. While

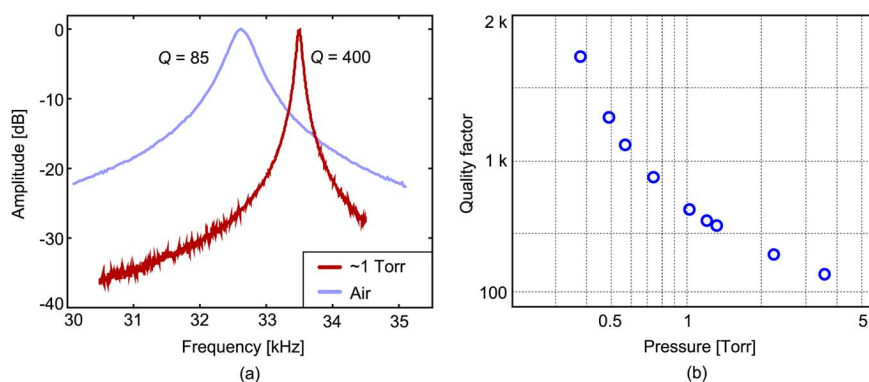


Fig. 8. (a) Frequency response of a cantilever with (red, $Q = 400$) and without (blue, $Q = 85$) vacuum packaging. (b) Dependence of quality factor (Q) on air pressure measured inside a vacuum chamber. At a pressure of ~ 1 torr, Q reaches a value that is characteristic of the devices with on-chip vacuum.

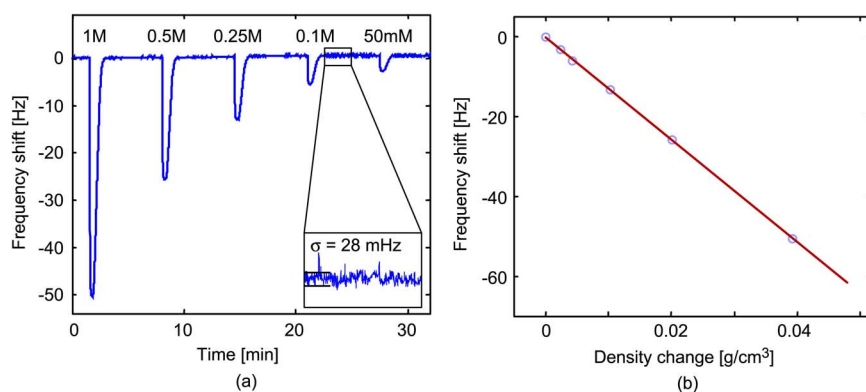


Fig. 9. (a) Frequency shift in response to a dilution series of sodium chloride solution in water (concentration 1 M to 50 mM). (b) Peak frequency shift versus density corresponding to the injected sodium chloride solutions.

the long-term stability of the vacuum sealed devices was not investigated in this work, Sparks *et al.* have shown that glass frit bonded packages can provide stable vacuum levels for several years under accelerated aging conditions [28].

We did not detect any difference in quality factor between an air-filled and a water-filled resonator, and measurements with water-filled cantilevers inside a vacuum chamber show that quality factors of more than 10 000 are possible at a pressure in the ten millitorr range .

Application of pressure in excess of 300 psi using a special fixture led to failure of the glass frit bond, while the suspended silicon nitride channels remained intact.

B. Device Sensitivity

Quantitative measurements of protein binding with the suspended microchannel resonator require an accurate calibration. To characterize the relation between frequency shift and mass change, we filled the resonator with samples of known density while monitoring the resonance frequency. This procedure is analogous to the method employed by Enoksson *et al.* [29] and by Westberg *et al.* [30] for the calibration of microfabricated fluid densitometers. Fig. 9(a) shows the sensor response to injecting aqueous sodium chloride solutions of various concentrations into a flow stream of pure water. Each time a sample plug reached the resonator, the frequency dropped rapidly, equilibrated for a short time, and then returned to the initial level.

The slow tailing at the end of each injection is a common artifact in liquid chromatography caused by mixing and dilution in the tubes through which the sample is delivered.

Fig. 9(b) plots the maximum frequency shift versus solution density for the different salt concentrations. The slope of the linear fit in Fig. 9(b) represents a density sensitivity of 40 000 $\text{ppm}/(\text{g}\cdot\text{cm}^{-3})$, which translates into 0.8 $\text{ppm}/(\text{g}\cdot\text{cm}^{-2})$ when normalized by the channel height and by the internal surface area of the resonator.

Using the feedback configuration shown in Fig. 6 we achieved a frequency resolution of ~ 1 ppm in a 4 Hz bandwidth. While the short-term noise is dominated by the displacement sensor and amplifier noise, stability on the time scale of minutes is limited by external factors such as temperature fluctuations.

C. Detection of Protein Binding

We demonstrated the ability to detect biomolecular binding inside the suspended microchannel resonator by first functionalizing the sensor with avidin and subsequently measuring the mass increase due to binding of different biotin labeled proteins. Avidin was first coated onto the channel surface by non-specific adsorption from a 1 mg/mL solution in phosphate buffered saline (PBS, 10 \times diluted, pH 7.4). The resulting frequency shift vs. time after the injection is plotted in Fig. 10(a), with arrows labeling the times at which the sample loop was connected to

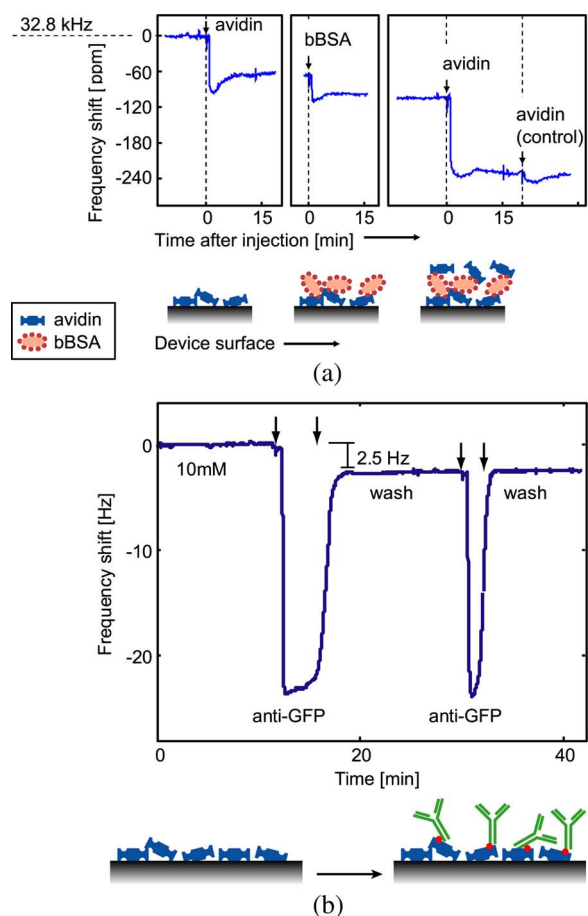


Fig. 10. (a) Avidin and biotinylated BSA are detected by the resonance frequency shift upon binding. The transient dip during the injections is due to the greater density of the sample compared to the running buffer. (b) Binding of biotin conjugated anti-GFP to avidin. The large transient signals result from a high salt concentration in the sample. After the first injection, a residual frequency shift of 2.5 Hz indicates binding of anti-GFP. A second injection verifies that the surface is saturated.

the device. Less than one minute after the injection, which corresponds to the time it took for the sample to flow from the injection valve to the sensor, the frequency dropped by about 90 ppm. Assuming a solution density of $1.3\text{--}1.4\text{ g/cm}^3$ for avidin, a concentration of 1 mg/mL would increase the bulk density of the buffer by $\sim 0.23 \cdot 10^{-3}\text{ g/cm}^3$, giving rise to a signal of only $\sim 10\text{ ppm}$. After the sample was rinsed out, the signal settled at an equilibrium value of -60 ppm , corresponding to a mass change of $\sim 75\text{ ng/cm}^2$, or, equivalently, $\sim 300\text{ ng/cm}^2$ adsorbed avidin if the density difference to water is taken into account. This is similar to reported values for the nonspecific adsorption of proteins on oxide surfaces. [31] The rise of the signal during rinsing can be explained by the difference in bulk density between the protein solution and the running buffer, and by loosely bound molecules detaching from the surface. After rinsing the device with PBS for more than 20 min, we injected biotin-conjugated bovine serum albumin (bBSA) which bound to the avidin present on the surface. The initial signal of $\sim 40\text{ ppm}$ exceeds the equilibrium value by 10 ppm, consistent with the density difference between the pure buffer and the bBSA solution. Again rinsing with PBS revealed the true mass change

due to the BSA attached to the surface. Since each molecule of BSA was labeled with 8-16 molecules of biotin it was possible to build up another layer of avidin molecules as illustrated in the last panel of Fig. 10(a).

We conducted several control experiments to ensure that the observed signals were indeed caused by specific binding of bBSA to avidin rather than being the result of non-specific adsorption or measurement artifacts. First, injecting solutions without proteins never resulted in a permanent change of the baseline, indicating that the signal was robust to disturbances caused by the switching. Second, specificity was verified by repeating the experiment with non-biotinylated BSA in place of bBSA, leading to no detectable mass signal. The same behavior resulted after two consecutive injections of avidin, as shown in the last panel in Fig. 10(a): Only the first of the two sample plugs showed evidence of binding, while the second passed over the surface without leaving any deposits, presumably owing to a lack of available binding sites.

Physisorption of avidin is a simple and versatile method for surface functionalization. Fig. 10(b) shows the immobilization of biotin conjugated anti-GFP to an avidin coated device. The sample was injected twice to ensure complete saturation of the surface. The periods during which the sample passed through the resonator can be recognized by the large transient frequency shift caused by the higher density of the anti-GFP solution. The density of the sample was higher than the density of the buffer due to an increased salt concentration and due to the presence of a background of 10 mg/mL BSA. When rinsing out the anti-GFP solution the amount of bound protein could be identified by the difference in baseline before and after the experiment.

VI. CONCLUSION

Vacuum-packaged fluid-filled resonators enable resonant mass measurements in liquid with high-frequency resolution. This paper presents the fabrication and characterization of suspended microchannels that are vacuum encapsulated and connect to a standard liquid chromatography system via a microfluidic manifold. The suspended channels can be driven into resonance by an alternating electric field. The primary feature that sets this work apart from research in the area of vibrating tube densitometers is that molecules that bind to the channel walls are detected, thereby providing a path to specificity via molecular recognition by immobilized receptors. High-surface sensitivity is achieved by making the resonator walls and the fluid layer very thin. The sensitivity of resonance frequency to a uniformly distributed mass is, to first order, independent of the resonator geometry.

Devices with a large surface-to-mass ratio were fabricated using low-stress LPCVD silicon nitride as structural material and polysilicon as a sacrificial layer. The completed resonators were vacuum packaged on the wafer-scale by glass frit bonding, resulting in mechanical quality factors in the range of 300–700. We expect that improving the vacuum level by incorporating on-chip getters will ultimately yield Q 's as high as 10 000. In comparison, the quality factor of cantilever resonators submerged in water is typically in the range of 1–10. To our knowledge, the highest quality factors for resonant biological sensors have so far been demonstrated with flexural plate wave

(FPW) and film bulk acoustic resonators (FBAR), which can attain a Q of 40–140 when operated in fluid. [17], [32]

Using suspended microfluidic channels with 800 nm thick walls and a 1- μm -fluid layer we measured a surface mass sensitivity of 0.8 ppm/(ng · cm²) and a noise equivalent mass loading of ~ 1 ng/cm² in a 4 Hz bandwidth. Estimations of the thermomechanical frequency noise suggest that, in principle, it should be possible to resolve adsorbed mass on the order of 0.01 ng/cm², which would be equivalent to fluorescence detection. In practice, further refinements of the readout circuitry are needed to achieve this resolution. Furthermore, differential sensing will be required to maintain long-term stability in assays with slow binding kinetics and to suppress signals from non-specific interactions when measuring complex mixtures. Macroscopic quartz crystal microbalances, in comparison, can resolve mass changes of ~ 1 ng/cm² in liquid, [4] and surface plasmon resonance, which is the most widely employed label-free detection technology today, has a resolution of ~ 0.05 ng/cm². [33]

While scalability is currently constrained by the optical readout of our resonator, this is not a fundamental limitation, as methods such as capacitive or piezoelectric sensing could replace the optics without significantly increasing the complexity of the fabrication process. A potential drawback of using very thin and long fluidic channels for affinity detection is that dilute target molecules could get depleted from the solution more quickly than they are replenished by the flow. Increasing the channel height can effectively eliminate this problem at the expense of a small decrease in mass sensitivity. Using the analytical and numerical models outlined in [25], future projects could address the optimization of the channel height to provide maximum sensitivity under application dependent constraints on sample consumption and analyte depletion.

In summary, suspended microchannel resonators are an attractive technology for the label-free detection of biological molecules in liquid because of their high sensitivity and low-sample consumption. We have demonstrated the batch fabrication and wafer-scale vacuum packaging of these sensors using standard silicon and glass micromachining processes. Suspended microchannel resonant mass sensors may be readily integrated with microfluidic sample preparation, and ultimately we envision that a combined system could enable experiments in cell biology that are not feasible with existing bioanalytical techniques.

ACKNOWLEDGMENT

The authors thank K. Babcock and D. Rugar for helpful discussions.

REFERENCES

- [1] J. Homola, S. S. Yee, and G. Gauglitz, "Surface plasmon resonance sensors: review," *Sens. Actuators B, Chem.* vol. B54, pp. 3–15, Jan. 25, 1999 [Online]. Available: [http://dx.doi.org/10.1016/S0925-4005\(98\)00321-9](http://dx.doi.org/10.1016/S0925-4005(98)00321-9)
- [2] Biacore AB. Uppsala, Sweden [Online]. Available: <http://www.biacore.com>
- [3] P. Skladal, "Piezoelectric quartz crystal sensors applied for bioanalytical assays and characterization of affinity interactions," *J. Brazilian Chem. Soc.*, vol. 14, pp. 491–502, Jul.–Aug. 2003.

- [4] Q-Sense AB. Västra Frölunda, Sweden [Online]. Available: <http://www.q-sense.com>
- [5] J. Fritz, E. B. Cooper, S. Gaudet, P. K. Sorger, and S. R. Manalis, "Electronic detection of DNA by its intrinsic molecular charge," *Proc. Nat. Acad. Sci. U.S.A.*, vol. 99, pp. 14142–14146 ER, Oct. 29, 2002.
- [6] Y. Cui, Q. Q. Wei, H. K. Park, and C. M. Lieber, "Nanowire nanosensors for highly sensitive and selective detection of biological and chemical species," *Science*, vol. 293, pp. 1289–1292, Aug. 17, 2001.
- [7] J. Voros, J. J. Ramsden, G. Csucs, I. Szendro, S. M. De Paul, M. Textor, and N. D. Spencer, "Optical grating coupler biosensors," *Biomaterials*, vol. 23, pp. 3699–3710, Sep. 2002.
- [8] W. Lukosz, "Integrated-optical biosensors," *Abstr. Papers Amer. Chem. Soc.*, vol. 213, p. 210-ANYL, Apr. 13, 1997.
- [9] M. A. Cooper, "Optical biosensors in drug discovery," *Nature Rev. Drug Discovery*, vol. 1, pp. 515–528, Jul. 2002.
- [10] J. Fritz, M. K. Baller, H. P. Lang, H. Rothuizen, P. Vettiger, E. Meyer, H. J. Guntherodt, C. Gerber, and J. K. Gimzewski, "Translating biomolecular recognition into nanomechanics," *Science*, vol. 288, pp. 316–318, Apr. 14, 2000.
- [11] G. H. Wu, R. H. Datar, K. M. Hansen, T. Thundat, R. J. Cote, and A. Majumdar, "Bioassay of prostate-specific antigen (PSA) using microcantilevers," *Nat. Biotechnol.*, vol. 19, pp. 856–860, Sep. 2001.
- [12] C. A. Savran, T. P. Burg, J. Fritz, and S. R. Manalis, "Microfabricated mechanical biosensor with inherently differential readout," *Appl. Phys. Lett.*, vol. 83, pp. 1659–1661, Aug. 25, 2003.
- [13] T. Thundat, E. A. Wachter, S. L. Sharp, and R. J. Warmack, "Detection of mercury-vapor using resonating microcantilevers," *Appl. Phys. Lett.*, vol. 66, pp. 1695–1697, Mar. 27, 1995.
- [14] D. Lange, C. Hagleitner, A. Hierlemann, O. Brand, and H. Baltes, "Complementary metal oxide semiconductor cantilever arrays on a single chip: mass-sensitive detection of volatile organic compounds," *Anal. Chem.*, vol. 74, pp. 3084–3095, Jul. 1, 2002.
- [15] B. Ilic, H. G. Craighead, S. Krylov, W. Senaratne, C. Ober, and P. Neuzil, "Attogram detection using nanoelectromechanical oscillators," *J. Appl. Phys.* vol. 95, pp. 3694–3703, 2004 [Online]. Available: <http://dx.doi.org/10.1063/1.1650542>
- [16] R. M. White and S. W. Wenzel, "Fluid loading of a lamb-wave sensor," *Appl. Phys. Lett.*, vol. 52, pp. 1653–1655, May 16, 1988.
- [17] M. S. Weinberg, C. E. Dube, A. Petrovich, and A. M. Zapata, "Fluid damping in resonant flexural plate wave device," *J. Microelectromech. Syst.*, vol. 12, pp. 567–576, Oct. 2003.
- [18] C. K. O'Sullivan and G. G. Guilbault, "Commercial quartz crystal microbalances—theory and applications," *Biosens. Bioelectron.*, vol. 14, pp. 663–670, Dec. 1999.
- [19] B. Ilic, Y. Yang, and H. G. Craighead, "Virus detection using nanoelectromechanical devices," *Appl. Phys. Lett.* vol. 85, pp. 2604–2606, 2004 [Online]. Available: <http://dx.doi.org/10.1063/1.1794378>
- [20] A. W. Wang, R. Kiwan, R. M. White, and R. L. Ceriani, "A silicon-based ultrasonic immunoassay for detection of breast cancer antigens," *Sens. Actuators B, Chem.*, vol. 49, pp. 13–21, Jun. 25, 1998.
- [21] T. P. Burg and S. R. Manalis, "Suspended microchannel resonators for biomolecular detection," *Appl. Phys. Lett.* vol. 83, pp. 2698–2700 [Online]. Available: <http://dx.doi.org/10.1063/1.1611625>
- [22] J. Tsai, R. Taylor, C. Chothia, and M. Gerstein, "The packing density in proteins: standard radii and volumes," *J. Mol. Biol.*, vol. 290, pp. 253–266, Jul. 2, 1999.
- [23] J. Voros, "The density and refractive index of adsorbing protein layers," *Biophys. J.*, vol. 87, pp. 553–561, Jul. 2004.
- [24] C. A. Savran, S. M. Knudsen, A. D. Ellington, and S. R. Manalis, "Micromechanical detection of proteins using aptamer-based receptor molecules," *Anal. Chem.*, vol. 76, pp. 3194–3198, Jun. 1, 2004.
- [25] T. Gervais and K. F. Jensen, "Mass transport and surface reactions in microfluidic systems," *Chem. Eng. Sci.* vol. 61, pp. 1098–1117, 2006.
- [26] M. B. Stern, M. W. Geis, and J. E. Curtin, "Nanochannel fabrication for chemical sensors," *J. Vacuum Sci. Technol. B (Microelectron. Nanometer Struct.)*, vol. 15, pp. 2887–2891, November 1997.
- [27] J. Tamayo, "Study of the noise of micromechanical oscillators under quality factor enhancement via driving force control," *J. Appl. Phys.*, vol. 97, p. 044903, Feb. 15, 2005.
- [28] D. Sparks, S. Massoud-Ansari, and N. Najafi, "Long-term evaluation of hermetically glass frit sealed silicon to Pyrex wafers with feedthroughs," *J. Micromech. Microeng.*, vol. 15, pp. 1560–1564, August 2005.
- [29] P. Enoksson, G. Stemme, and E. Stemme, "Vibration mode investigation of a resonant silicon tube structure for use as a fluid density sensor," in *Proc. 1995 IEEE Micro Electro Mechanical Syst.*, 29 Jan.–2 Feb. 1995, pp. 133–138.

- [30] D. Westberg, O. Paul, G. I. Andersson, and H. Baltes, "A CMOS-compatible device for fluid density measurements," in *Proc. IEEE The Tenth Annu. Int. Workshop on Micro Electro Mechanical Syst. An Investigation of Micro Structures, Sensors, Actuators, Machines and Robots*, Jan. 26–30, 1997, pp. 278–283.
- [31] K. Nakanishi, T. Sakiyama, and K. Imamura, "On the adsorption of proteins on solid surfaces, a common but very complicated phenomenon," *J. Biosci. Bioeng.* vol. 91, pp. 233–244, 2001 [Online]. Available: [http://dx.doi.org/10.1016/S1389-1723\(01\)80127-4](http://dx.doi.org/10.1016/S1389-1723(01)80127-4)
- [32] H. Zhang and E. S. Kim, "Micromachined acoustic resonant mass sensor," *J. Microelectromech. Syst.* vol. 14, pp. 699–706, Aug. 2005 [Online]. Available: <http://dx.doi.org/10.1109/JMEMS.2005.845405>
- [33] D. G. Myszka, "Analysis of small-molecule interactions using Biacore S51 technology," *Anal. Biochem.*, vol. 329, pp. 316–323, Jun. 15, 2004.



Thomas P. Burg (S'00–M'06) received the Dipl.-Phys. degree in physics from the Swiss Federal Institute of Technology (ETH), Zurich, in 2001 and the Ph.D. degree in electrical engineering and computer science from the Massachusetts Institute of Technology (MIT), Cambridge, in 2005.

His research at ETH Zurich involved the recognition of volatile organic compounds with capacitive microsensors, and his doctoral work at MIT focused on the development of micromechanical transducers for biological measurements. He is currently a Research Associate in the Division of Biological Engineering at MIT. His current research interests include the application of microtechnologies in chemistry and biology, and the design, fabrication, and packaging of microfluidic systems.

research Associate in the Division of Biological Engineering at MIT. His current research interests include the application of microtechnologies in chemistry and biology, and the design, fabrication, and packaging of microfluidic systems.



Amir R. Mirza received the Ph.D. degree in electrical engineering from the University of Sheffield, U.K., in 1984.

He has been involved in the MEMS industry for over 17 years, his extensive MEMS experience includes the development of a wide variety of silicon micromachined products—such as accelerometers, gyros, pressure sensors, optical MEMS and microfluidic devices. He has held engineering and management positions with Fortune 100 companies including Honeywell, Motorola, and GE. At GE

NovaSensor, he served as Director of Advanced Technologies responsible for R&D for both MEMS design and process development. He is currently an International Product Manager for SUSS MicroTec in Waterbury, Vermont. He joined SUSS MicroTec from Innovative Micro Technology, Santa Barbara, CA, a leading MEMS design and fabrication foundry, where he held program management responsibilities for new product introductions.



Nebojsa Milovic received the B.S. degree in chemistry from Belgrade University, Belgrade, Serbia, in 1997 and the Ph.D. degree in chemistry from Iowa State University, Ames, in 2002.

He is currently a Postdoctoral Associate with the Division of Biological Engineering at the Massachusetts Institute of Technology (MIT), Cambridge, and his research interest is focused on development of label-free microfluidic biosensors for medical and environmental applications.



Christine H. Tsau received the S.B. and Ph.D. degrees in materials science and engineering from the Massachusetts Institute of Technology (MIT), Cambridge, in 1998 and 2003, respectively.

She was a Postdoctoral Associate at MIT's Biological Engineering Division from 2003 to 2005, where her research focused on bioMEMS devices. Currently, she is a Sr. Packaging Engineer at Intel Corporation, Chandler, AZ.



George A. Popescu received the Engineer Diploma and a Master of Sciences Diploma from Ecole Supérieure d'Electricité (Supélec) in Gif-sur-Yvette, France, in 2005. He is working towards the Master of Sciences degree at the Massachusetts Institute of Technology (MIT), Cambridge, Media Laboratory.

His research interests are digital fabrication of active micrometer scale structures, programmable self assembly of microstructures, synthetic biology, and number theory.



John S. Foster was born in Berkeley, CA, on September 20, 1958. He received the Bachelor's degree in physics from the University of California, San Diego, in 1980 and the Ph.D. degree in applied physics from Stanford University, Stanford, CA, in 1984.

He was formerly a faculty member at Stanford University. Thereafter, he was employed at IBM as an R&D manager then a product manager. He later joined Applied Magnetics Corporation as the Plant General Manager in Malaysia. He was promoted to

the position of COO. In 2000, he co-founded Innovative Micro Technology (IMT) and is currently the CEO and the chairman of the board. He holds 19 U.S. patents with the most recent one in MEMS cell sorter technology. He also co-invented the near-contact recording for storage disk drives, made the first real-space observation of individual molecules (using scanning tunneling microscopy), and made the first measurement of zero-point motion amplification in Superfluid Helium-4.



Scott R. Manalis received the B.S. degree in physics from the University of California, Santa Barbara, in 1994 and the Ph.D. degree in applied physics from Stanford University, Palo Alto, CA, in 1998.

He is currently an Associate Professor in Biological and Mechanical Engineering at the Massachusetts Institute of Technology (MIT), Cambridge. His research group applies microfabrication technologies towards the development of novel methods for probing biological systems. Current projects focus on using electrical and mechanical detection schemes for analyzing DNA, proteins and cell.

Dr. Manalis was the recipient of the Presidential Early Career Award for Scientists and Engineers (PECASE) from the Department of Defense. He has also been selected by *Technology Review* magazine as one of the 100 innovators under the age of 35 whose work and ideas "will have a deep impact on how we live, work and think in the century to come."